

CALIBRATION OF AN AEROSOL LIDAR OPERATING IN PHOTON COUNTING REGIME AND DETECTION OF ATMOSPHERIC INHOMOGENEITIES

S.M. Pershin, A.V. Bukharin, V.M. Linkin, and V.S. Makarov

Space Research Institute,
the Russian Academy of Sciences, Moscow
Received January 17, 1994

In this paper we present a technique for calibration of a lidar emitting into the atmosphere sounding pulses of micro-Joule energy that allows for the purely statistical nature of return signals (recorded in the photon counting mode). Some results of measurements of the backscattering coefficient in the atmosphere up to several hundred meters are presented and the capability of the lidar to detect invisible atmospheric inhomogeneities is demonstrated. Prospects of using such an eye-safe lidar in the environmental monitoring avoiding damage from laser radiation is discussed.

INTRODUCTION

Theoretical analysis of a lidar operating in the photon counting mode shows principle possibility of its eye-safe operation in a kilometer range, when the probability of recording a signal during one laser shot is well below unity.^{1,2} To obtain a statistically significant result it is necessary to use a great number of laser shots in this mode of lidar operation. That brings some peculiarities to the process of measuring the physical parameters of a medium under study. The account of these peculiarities is necessary, first of all, for making a correct calibration of the lidar.

There are two most widely used calibration techniques, one uses Rayleigh scattering in the stratosphere³ at heights of 25–30 km and another one uses target with known albedo^{4,5}. The latter is more convenient for use in our experiment. The results of calibration of the lidar operating in the photon counting mode allowed us to obtain the backscattering coefficient profile when sounding the inhomogeneous atmosphere. Just these results made a subject for discussion in this paper.

LIDAR

Lidar prototype was constructed following a classic bistatic scheme with spaced transceiving channels. It consists of an optical unit, electronic control unit and a system of data processing and displaying based on a microcomputer.

A semiconductor pulsed laser is used in our lidar as a light source. The output beam of the lidar transmitter is formed with a lens objective. A typical shape of the laser pulse is shown in Fig. 1 together with the fragment of its leading edge. The quick change of the light power at the beginning of the laser pulse with a quick (less than 1 ns) increase time and a stable delay from the triggering pulse (less than 0.5 ns) makes it possible to measure the delay of the laser pulse along the path with high accuracy. The dependence of the relative power and the pulse duration on temperature within the range from –20 to 50°C is shown in Fig. 2. Insignificant variations of the laser pulse power and duration allow the operation under normal conditions without special stabilization of the laser temperature.

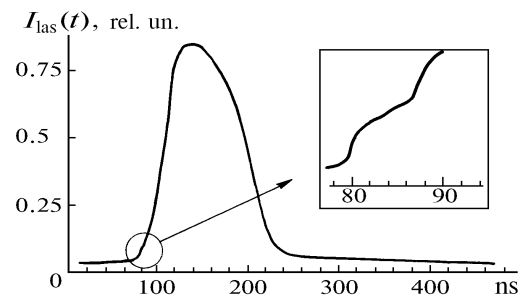


FIG. 1. Typical shape of the laser pulse with the fragment of its leading edge.

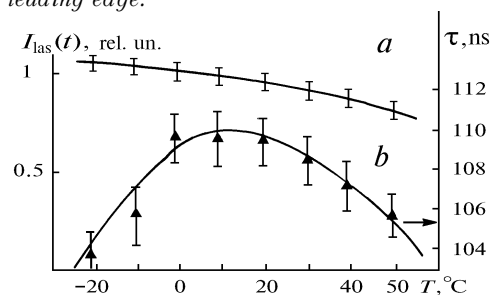


FIG. 2. Relative power and duration of the laser pulse as a function of temperature within the range from –20 to 50°C.

Specifications of the lidar transmitter are given in Table I together with the range of their possible variations that can occur when changing a laser.

TABLE I. Specifications of the lidar transmitter.

energy per pulse	0.4–1 μ J
pulse duration	70–110 ns
wavelength*/line width	850– 910 nm/1 nm
pulse repetition frequency	up to 20 kHz
emitting area size	1000 \times 2 μ m
diameter of output aperture/divergence	40 mm/10 \times 1 mrad

* The laser ($\lambda = 884.3$ nm, pulse power of 0.5 μ J) operating with frequency 2.5 kHz was mounted in the lidar prototype.

The detection of lidar returns is performed with an avalanche photodiode of silicon that had a picosecond response time, low level of internal noise and the inner amplification factor up to 10^9 . Figure 3 shows a typical temperature behavior of the detector dark current pulses count rate (ω_n), photosensitive area of the detector being $100 \mu\text{m}$ in diameter. It is seen from this figure that even at temperature -50°C the dark current count rate of the detector does not exceed 10 kHz. It corresponds to the noise level of the detector with the diameter $40 \mu\text{m}$ at room temperature. Such a low noise level at room temperature makes it possible the operation of a detector in the photon counting mode without cooling the photodetector, if a time gating is performed by pulses with the duration less or equal to the period between the noise pulses. The scanning along the path is realized by moving the strobe along the time axis.

Specifications of the receiving channel are given in Table II.

TABLE II. Specifications of the receiving channel.

diameter of a photosensitivity spot	20 μm ; 40 μm ; 100 μm
wavelength range	0.36 – 1.1 μm
quantum efficiency at 850 nm	23%
voltage of the avalanche break	18–33 V
dark current count rate at 20°C and the voltage of 0.7 V above the avalanche break threshold	< 30 Hz; < 10 kHz; < 300 kHz
aperture of the objective field of view*	16 mm 1 mrad
interference filter: band/transmittance wavelength	8 nm/70% 884 nm

* In the lidar version discussed here the field of view of the receiver intercepts only 1/10 of sounding beam.

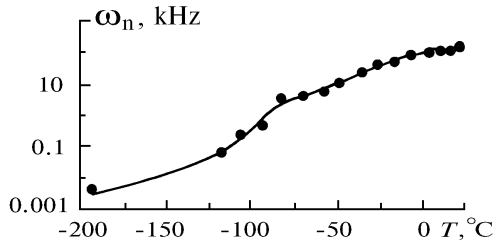


FIG. 3. Count rate of the detector dark current as a function of temperature. The diameter of the detector sensitive area is $100 \mu\text{m}$.

The transceiving channels of the lidar are mounted on a common base of the lidar optical block at a 75 mm spacing between the optical axes that provided their mutual alignment. The optical block is connected via a cable with the interface block and then with a computer. The lidar mass without a computer does not exceed 2 kg depending on the configuration. Total energy consumed is about 5 W that makes it possible to use battery with small capacity in a shipborne variant. The lidar operation range is several kilometers depending on the sky background level and the atmospheric transparency.

As it follows from the consideration of the main principles of lidar operation,² the field of its application can be very diverse. In this paper we present the results which illustrate the possibilities of using this lidar in the environmental monitoring. For example, it is the detection

of the local sources of aerosol pollution (dust, smoke, etc.). When sounding the atmosphere of the corridor the invisible dust of enhanced content was detected in the lift hall. A monotonic increase of the aerosol pollution of the atmosphere of the corridor of the passenger ship "Il'ya Repin" was detected from stern to the music hall in the front part of the ship.

CALIBRATION OF THE LIDAR

Calibration of the lidar was carried out in order to obtain quantitative estimates of the parameters of the profile of backscattering coefficient along the sounding path. Calibration was carried out using a signal from a target surface^{4,5} taking into account the specific peculiarities of the lidar detector operation in the photon counting mode and representation of data in a histogram form.²

Let us write the lidar equation⁵ in terms of photocounts caused by scattering of the laser pulse by an atmospheric layer with the thickness dx taking no into account the absorption along the sounding path

$$N(\Omega_i; x) = \eta \Phi N \beta \frac{S}{x^2} O(x) dx, \tag{1}$$

where η is the efficiency of the optical receiver; $N \times \Phi$ is the total number of the photons emitted by the transmitter into the atmosphere in N laser shots; β is the atmospheric backscattering coefficient; $O(x)$ is the geometrical function of the lidar that characterizes overlapping of the receiver field of view and the laser beam at a distance x from the lidar;⁵ and, S is the area of the input aperture of the optical receiver.

By integrating Eq. (1) we find the number of photons scattered by an atmospheric layer at a distance L and $c\tau/2$ thick, where τ is the duration of a time gate, the strobe T is divided, c is the light speed

$$N(\Omega_i; L) = \eta \Phi N S \beta \int_L^{L+c\tau/2} \frac{dx}{x^2} O(x) = \eta \Phi N \beta S O(L) \int_L^{L+c\tau/2} \frac{dx}{x^2} = \eta N \Phi S \bar{O}(L) \beta \frac{c \tau / 2}{L(L + c \tau / 2)},$$

$$N(\Omega_i; L) = \eta N \Phi \beta S \bar{O}(L) \frac{c \tau / 2}{L(L + c \tau / 2)}, \tag{2}$$

$\bar{O}(L)$ is the average value of the lidar geometric function along the layer at a distance from L to $L + c\tau/2$.

Then the total number of photocounts at the signal maximum is determined by the following expression when detecting the photons scattered by a surface placed at the distance R :

$$N^{(1)}(\Omega_i) = \eta \rho \Phi N^{(1)} \frac{S^{(1)}}{R^2} O(R). \tag{3}$$

The index (1) denotes the number of counts obtained in the experiment on lidar calibration by a signal from a target surface; ρ is the scattering coefficient of the target surface.

The difference between the expressions (2) and (3) is caused by the peculiarities of signal formation at scattering of photons in an extended layer and by a plane surface.

Let us find the ratio of Eq. (2) to Eq. (3)

$$\frac{N(\Omega_1; L)}{N^{(1)}(\Omega_1)} = \frac{\beta}{\rho} \frac{S}{S^{(1)}} \frac{N}{N^{(1)}} \frac{\bar{O}(L)}{O(R)} \frac{R^2 c \tau}{2(L+c \tau / 2) L} \quad (4)$$

Then we obtain the expression for calculating the backscattering coefficient β

$$\beta = \rho \frac{N(\Omega_1; L) N^{(1)}}{N^{(1)}(\Omega_1) N} \frac{S^{(1)}}{S} \frac{O(R)}{\bar{O}(L)} \frac{2 L(L+c \tau / 2)}{R^2 c \tau} \quad (5)$$

Note that when calibrating the lidar it is necessary to use a target with a minimum possible component of specular reflection in order to make use of the Lambertian law for surface reflection. It is known⁴ that the albedo σ of the Lambertian surface and the scattering coefficient ρ are connected by the relationship $\rho = \sigma/\pi$, where σ is measured by means of a calibrated device. One should be careful when taking into account the effects connected with the difference of the directional patterns of different targets from the Lambertian one, because it can give a significant contribution to the error of backscattering coefficient measurements.⁵

During the calibration experiment, first the signal and the background histograms were compiled and then preliminary processing of histograms was performed in an automatic mode including the linearization procedure and representation of data in the form corresponding to the detector with zero dead time.² After processing histograms the average number of signal photocounts in the strobe was calculated for the counter with zero dead time $P(\Omega_1)$. As a result, the dependencies of $P(\Omega_1)$ on the scattering coefficient ρ and the distance R from the target were obtained. The latter dependence in our case is proportional to the geometric function $O(R)$, see Ref. 5. The geometric function of the lidar used reaches its plateau at 50 m. In this case $O(R) = O(L)$ for R and $L \gg 50$ m.

The sought calibration dependence of $P(\Omega_1)$ on ρ is depicted in Fig. 4. It was obtained at three distances for two kinds of sand-papers with the reflection coefficients 0.16 and 0.32 at the laser wavelength. A straight line determined by the regression analysis technique was drawn through the experimental points, then the proportionality factor was calculated for the expression $P(\Omega_1) = \alpha\rho$ as well as its error $\Delta\alpha$. As a rule, in the experiment $\Delta\alpha/\alpha > 0.1$, what makes an actual error in the coefficient ρ in Eq. (5). Eventually it determines the accuracy of the backscattering coefficient measurements. The spread of $\Delta\alpha$ values is mainly determined by deviations of an actual surface reflection diagram from the Lambertian one and by the accuracy with which the target surface is installed perpendicularly to the lidar beam.

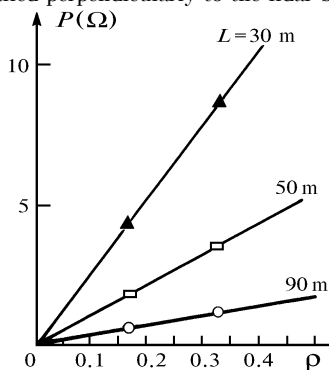


FIG. 4. Average number of events recorded in the strobe as a function of the surface scattering coefficient ρ .

In our case the average value of the coefficient α measured at distances 30, 50, and 90 m was 1.3, 0.57, and 0.17, respectively, for the number of laser shots $N = 32\,000$ in each series.

Thus obtained calibration data enabled the calculation of the instrumental constant of the lidar.⁵ Calculations have been made using the 5th channel data by formula

$$\beta = K \frac{N_5(\Omega_1)}{N}; \quad K = [\text{m}^{-1} \cdot \text{sr}^{-1}] = 1.2 \cdot 10^{-3}, \quad (6)$$

where $N_5(\Omega_1)$ is the number of counts in the 5th channel of the reconstructed histogram during N laser shots.

The analysis of the factors that determine the accuracy of the physical parameters measurements by means of the lidar discussed will be considered in further publications.

Let us turn our attention to the results on the measuring backscattering coefficient of the atmosphere. One should note some above-mentioned peculiarities in the formation of the backscattering signal histogram, depending on the object sounded. It is known that a signal response from a transparent layer irradiated with a laser pulse is wider in duration than the laser pulse by the amount equivalent to the layer thickness. Thus, in the case of a semi-infinite homogeneous medium with a plane boundary, like cloud base, fog, stack plume, and so on, the leading edge of a response signal has the duration approximately equal to the sounding pulse duration, while the trailing edge of the response will have a duration that is determined by the value of the extinction coefficient of the medium.^{5,7}

Let us note that if the layer thickness x is essentially greater than $c\tau$, where τ is the laser pulse duration, and the backscattering coefficient β only weakly varies along a path into the layer, $\beta(x, x + c\tau)/\beta(x) < 1$, then starting from some distance, one should use the maximum value of a signal against the background in a separate histogram channel in order to estimate β . In other case, when the layer width is less than $c\tau$, one should use the total number of counts within the signal maximum on a histogram for $N(\Omega_1, L)$, as in the case of scattering by a surface used for calibration or measuring its albedo.

Further, when calculating the backscattering coefficient profile in the atmosphere in presence of weakly absorbing layers on the sounding path we shall use the maximum number of signal counts against the background in a separate channel of the signal peak on the histogram.

SOUNDING OF THE ATMOSPHERE

In order to experimentally test the lidar complex it was necessary to measure the backscattering coefficient profile in a homogeneous atmosphere along a path with no local sources of the atmospheric inhomogeneities. In our opinion, the most useful place for such an experiment is the atmosphere over a vast water surface, at a certain distance from the coast. The homogeneity of the parameters over extended surfaces provides the stationarity of the processes in the near surface atmospheric layer.⁷ The night is also favorable for such an experiment since the effects of solar radiation on the atmospheric layers decrease and the level of the background noise and its fluctuations has also low intensity. The favorable meteorological conditions allowed us to conduct such an experiment during the ecological expedition onboard the ship "Il'ya Repin" en route Moscow-Nizhny Novgorod-Moscow when passing through the Gorky water storage at night on July 2 – July 3, 1993. The lidar was mounted on the upper deck of the ship at the height of 13 m above the water surface. Sounding of the

atmosphere was carried out along a horizontal path perpendicularly to the ship board. The ship speed was ~ 20 km/h. Continuous ship movement allowed us to obtain the experimental values averaged over the route sections of 0.1 to 2 km length, depending on the measurement time. The possibility of such an averaging as well as high transparency of the atmosphere and the absence of noticeable wind flows allowed us to expect a good reproducibility of experimental data.

Typical histograms of the distribution of the signal counts due to backscattering of laser pulses in the atmosphere are shown in Figs. 5a and b without a correction for distance. Return signal shown in Fig. 5a has been obtained from 1 024 000 laser shots and that in Fig. 5b from 512 000 shots.

One can see from the figures that:

1) backscattering signal reaches its maximum at 25 m from the lidar and monotonically decreases with increasing distance. As this takes place, the amplitude and the contrast of the signal maximum are comparable with the backscattering signal obtained by the lidar with the pulse energy up to 5 mJ (see Ref. 9) that is 10 000 times greater than the laser pulse energy in our lidar;

2) histograms have only one distinct signal maximum, that is indicative of the homogeneity of the atmosphere, at least within 300-m long layer;

3) the maximum number of photocounts and the sum of the signal photocounts are proportional to the number of laser shots. This demonstrates the possibility of applying the approximation of stationarity of the atmospheric processes over the water storage surface, which weakly change during the total time (10 min) of the lidar data collection.

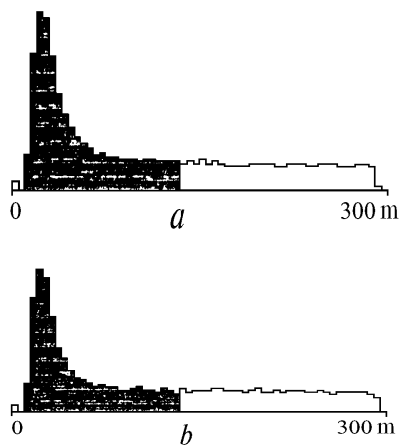


FIG. 5. Typical shape of "signal + noise" histograms when sounding homogeneous atmosphere over the Gorky water storage at night on July 2 to July 3, 1993 for the following numbers of laser shots: 1 024 000 (a) and 512 000 (b), total numbers of counts over the dashed areas are 36 694 and 17 682, respectively.

A comparison of the maximum values of count numbers from four successive measurement cycles showed that the sample value of the rms deviation exceeds its theoretical value only by 20% that is indicative of an actual value of the nonstationarity of the atmospheric optical properties during the measurements. The backscattering coefficient profile was calculated from the calibration of results⁶ along the first 300 m of the sounding path taking into account the correction for the squared range factor. It was shown that the value of the backscattering coefficient

was constant in this section of the Gorky water storage and was equal to $(4 \pm 1) \cdot 10^{-6} \text{ m}^{-1} \text{ sr}^{-1}$.

It should be noted that the absence of any additional signal within the first 300 m of the path can be caused not only by homogeneity of the atmosphere but also by possible misalignment of the transceiving channels of the lidar. To check this assumption we have decided immediately to carry out a sounding of the atmosphere along a path where distinct inhomogeneities are observed. The corridor of the second deck of the ship "Il'ya Repin" was selected for this experiment. It passes through a small and big staircase halls and ends at the music and dancing hall in the bow part at the distance of 50 m from the lidar.

The sounding scheme in the direction from the ship stern to the bow is shown in Fig. 6 as well as the results of measuring the profile of the backscattering coefficient along this path at 2 a.m. on July 3, 1993. Note, that in general, the aerosol pollution of air in the corridor is 2 to 4 times greater than in the open air. Thus the first measurement of the backscattering coefficient profile, shown by squares in the figure, shows that the atmosphere in the corridor near rooms is relatively clear while the atmosphere with higher content of aerosol dust, tobacco smoke and so on is observed near the main staircase hall and music hall. The dust content in the atmosphere quickly increased after a few people passed along the corridor. It was readily seen by an increase of the backscattering signal (circles in Fig. 6) in subsequent measurements after averaging over three measurement cycles.

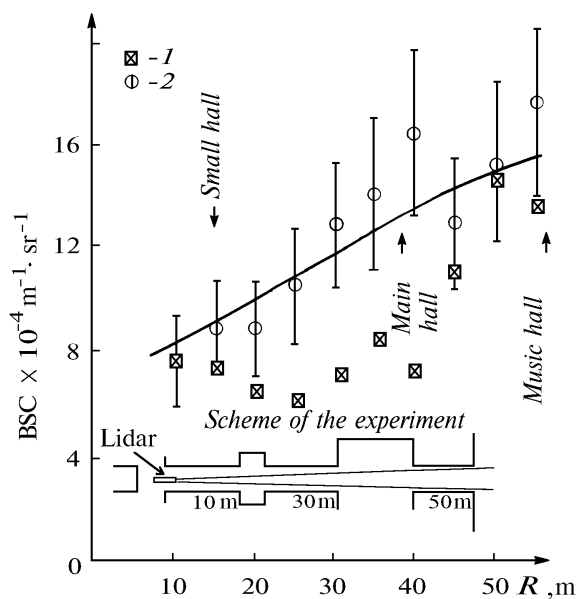


FIG. 6. Backscattering coefficient profile along the corridor of the ship "Il'ya Repin" at 2 a.m. on July 3, 1993: 1) the result of single measurement of the backscattering coefficient profile; 2) the backscattering coefficient profile averaged over three subsequent measurements after a few people passed along the corridor.

In order to check this technique of measuring the backscattering coefficient profile such an experiment was carried out in the corridor of the Space Research Institute of the Russian Academy of Sciences after coming back from the expedition. The scheme of measuring the backscattering coefficient profile is shown in Fig. 7 together with the results of its calculation from sounding data. The most

strong pollution of the atmosphere ($9 \cdot 10^{-6} \text{ m}^{-1} \text{ sr}^{-1}$) caused by maintenance works was observed in the second lift hall of the building at the end of the path at a distance of 100 m from the lidar. The dust content here was comparable with the aerosol pollution in the music hall of the ship "Il'ya Repin" at night on July 3, 1993. In the rest part of the corridor the backscattering coefficient value was more than one order of magnitude lower than in the lift hall, however no essential differences in the air transparency in different parts of the corridor were observed visually.

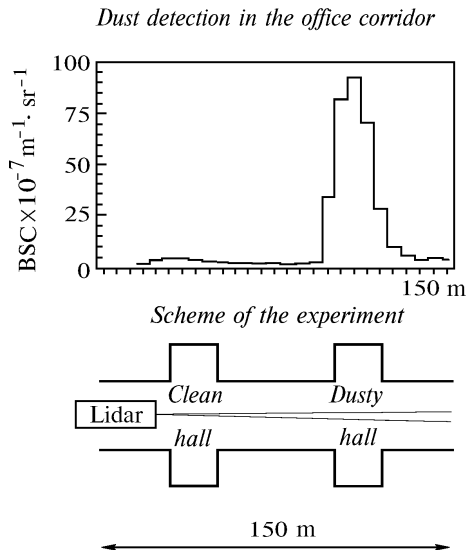


FIG. 7. Sounding scheme and calculational results on the backscattering coefficient (BSC) profile along the corridor at the Space Research Institute building.

In spite of the high backscattering coefficient value in the lift hall, the degree of atmospheric pollution here is less than in Zaporozhie city, where the authors of Ref. 5 have obtained the linear dependence of the aerosol mass density on the backscattering coefficient for its changes within the limits $(2-20) \cdot 10^{-5} \text{ m}^{-1} \text{ sr}^{-1}$. This enables us to estimate the maximum aerosol mass density (not more than $0.1 \mu\text{g}/\text{m}^3$, in our case). The minimum value of the backscattering coefficient was $5 \cdot 10^{-7} \text{ m}^{-1} \text{ sr}^{-1}$ in the middle part of the corridor (see Fig. 7) that is only few times greater than Rayleigh scattering coefficient of clear atmosphere¹⁰ ($2 \cdot 10^{-7} \text{ m}^{-1} \text{ sr}^{-1}$).

All this shows good possibilities of using a compact eye-safe lidar for the control of air quality inside building also.

Thus, the lidar described above is capable of detecting invisible aerosol and dust layers in the atmosphere with the effective backscattering cross section comparable with Rayleigh scattering of clear air. Given the particle size distribution function the mass density of aerosol pollution is an easily assessable value.

CONCLUSION

In this paper we described a technique for calibration of a lidar emitting into the atmosphere sounding pulses of micro-Joule energy. The detector of such a lidar operates in a purely statistical mode when signals are recorded in a photon counting regime. The calibration was carried out using a target surface taking into account some peculiarities in the formation of return signal. The possibility of measuring the backscattering coefficient profile is demonstrated as well as the possibility of detecting invisible atmospheric inhomogeneities along a sounding path up to several hundred meters. It is shown that the lidar under consideration is capable of obtaining the data not only on the average value of the optical parameters of the atmosphere during measurement period but also of estimating the nonstationarity degree of the spatial distribution of atmospheric aerosol along the sounding path.

The results obtained show that the eye-safe environmental laser monitoring is a new and the main field of application of such lidars.¹¹

REFERENCES

1. S. Pershin, V. Linkin, V. Makarov, I. Prochaska, and K. Hamal, in: *Proc. of the CLEO'91*, paper CFI 10, p. 120.
2. A. Bukharin and S. Pershin, *Atmos. Oceanic Opt.* **7**, No. 4, 521–537 (1994).
3. J. Rosen and T. Kjome, *Appl. Opt.* **30**, 1552–1561 (1991).
4. M. Kavaya and R. Menzies, *Appl. Opt.* **24**, 3444–3453 (1985).
5. V.E. Zuev, B.V. Kaul, I.V. Samokhvalov, et al., in: *Laser Sounding of Industrial Aerosols* (Nauka, Novosibirsk, 1986), 186 pp.
6. K. Sassen and G. Dodd, *Appl. Opt.* **17**, 3162–3165 (1982).
7. L.S. Ivlev and S.D. Andreev, *Optical Properties of Atmospheric Aerosols* (State University Publishing House, Leningrad, 1986), 360 pp.
8. V.S. Shamanaev, *Atmos. Oceanic Opt.* **5**, No. 7, 444–447 (1992).
9. P. Rairoux, J. Wolf, and L. Woste, *Appl. Opt.* **28**, 2052–2056 (1989).
10. E.J. McCartney, ed., *Optics of the Atmosphere* (Wiley, New York, 1977).
11. Yu.S. Balin and J.A. Rasenkov, *Atmos. Oceanic Opt.* **6**, No. 2, 104–114 (1993).